Biochimica et Biophysica Acta 1808 (2011) 2973–2980

Contents lists available at SciVerse ScienceDirect

Biochimica et Biophysica Acta

journal homepage: www.elsevier.com/locate/bbamem

The natural antioxidant rosmarinic acid spontaneously penetrates membranes to inhibit lipid peroxidation in situ

Ophélie Fadel [a], Karim El Kirat [b], Sandrine Morandat [a,*]

[a] Université de Technologie de Compiègne-CNRS, UMR 6022 Génie Enzymatique et Cellulaire, BP 20529, 60205 Compiègne Cedex, France
[b] Université de Technologie de Compiègne-CNRS, UMR 6600 BioMécanique et BioIngénierie, BP 20529, 60205 Compiègne Cedex, France

ARTICLE INFO

Article history:
Received 14 April 2011
Received in revised form 26 July 2011
Accepted 4 August 2011
Available online 12 August 2011

Keywords:
Biomimetic membrane
Oxidative stress
Rosmarinic acid
Antioxidant
Polyphenol
Lipid peroxidation

ABSTRACT

Exogenous molecules from dietary sources such as polyphenols are very efficient in preventing the alteration of lipid membranes by oxidative stress. Among the polyphenols, we have chosen to study rosmarinic acid (RA). We investigated the efficiency of RA in preventing lipid peroxidation and in interacting with lipids. We used liposomes of 1,2-dilinoleoyl-*sn*-glycero-3-phosphocholine (DLPC) to show that RA was an efficient antioxidant. By HPLC, we determined that the maximum amount of RA associated with the lipids was ~1 mol%. Moreover, by using Langmuir monolayers, we evidenced that cholesterol decreases the penetration of RA. The investigation of transferred lipid/RA monolayers by atomic force microscopy revealed that 1 mol% of RA in the membrane was not sufficient to alter the membrane structure at the nanoscale. By fluorescence, we observed no significant modification of membrane permeability and fluidity caused by the interaction with RA. We also deduced that RA molecules were mainly located among the polar headgroups of the lipids. Finally, we prepared DLPC/RA vesicles to evidence for the first time that up to 1 mol% of RA inserts spontaneously in the membrane, which is high enough to fully prevent lipid peroxidation without any noticeable alteration of the membrane structure due to RA insertion.

1. Introduction

In living organisms, the oxidative stress is associated with several physiopathological affections (e.g. atherosclerosis, cancer, aging, neurodegenerative diseases,…) [1]. The oxidative stress is generally associated with the generation of reactive oxygen and nitrogen species [1]. These highly reactive compounds have different molecular targets in cells: DNA, proteins and lipids [1,2]. Membrane lipids are not only constituents of an inert matrix but they are also mediators of several metabolic pathways [3,4]. Thus, the modification of lipids by reactive oxidant species can perturb different membrane-associated processes such as endo- and exo-cytosis, recognition by membrane receptors, activity of membrane enzymes, transport of metabolites and membrane–cytoskeleton interactions [5–8].

Such impairment of membrane functions has motivated the investigations of the factors that govern lipid peroxidation, but also of the protective role of antioxidants in membranes. Different endogenous and exogenous molecules can provide an efficient protection against lipid peroxidation: enzymes, vitamin E, cholesterol (Chol), plasmalogens and polyphenols [2,9–13]. Among the wide body of exogenous antioxidants, polyphenols constitute probably one of the most efficient classes of compounds against oxidative stress. Polyphenols are naturally available from various dietary sources, and they are increasingly recommended as a daily supplement to prevent oxidative stress [14–16]. Plants produce more than 8000 different polyphenols as secondary metabolites [17]. Chemically, polyphenols are compounds having one or more hydroxyl groups attached to a benzene ring. They can be categorized as flavonoids and non-flavonoid compounds. Flavonoids have a common C6–C3–C6 structure consisting of two aromatic rings (A and B) linked through a three carbon chain, usually organized as an oxygenated heterocycle (ring C) [17,18]. Flavonoids can be divided into several subfamilies according to the degree of oxidation of their oxygenated heterocycle. Among the non-flavonoid polyphenols, we can cite the stilbenes and the phenolic acids.

Because of the complexity of biological membranes, much work devoted to the efficiency of antioxidants on lipid peroxidation was performed with simplified lipid systems [12,13,19]. For example, by using DLPC liposomes, the flavonol quercetin was found to be a stronger inhibitor of lipid oxidation induced by UVB than by UVA [20]. Moreover different polyphenols such as curcumin and luteolin were also shown to be "super-active" antioxidants on the copper-induced peroxidation of liposomes composed of 1-palmitoyl, 2-linoleoyl-*sn*-glycero-3-phosphocholine and phosphatidylserine [21].

The ability of polyphenols to penetrate into lipid bilayers is undoubtedly crucial to the protection against oxidation. For polyphenols that partition in the non-polar region of the bilayer, they can inhibit the propagation of lipid oxidation by two mechanisms: (i) by intercepting intramembrane radicals and/or (ii) by increasing membrane fluidity, which disorganizes lipid chains and hinders radicals' propagation [22].

* Corresponding author at: Laboratoire de Génie Enzymatique et Cellulaire, UMR-CNRS 6022, Université de Technologie de Compiègne, BP 20529, 60205 Compiègne Cedex, France. Tel.: +33 3 44 23 44 18; fax: +33 3 44 20 39 10.
E-mail address: sandrine.morandat@utc.fr (S. Morandat).

0005-2736/$ – see front matter © 2011 Elsevier B.V. All rights reserved.
doi:10.1016/j.bbamem.2011.08.011

By contrast, Guttierez et al. showed a disordering effect of the citrus and rosemary phenolic extracts on the lipid membrane of a bovine brain extract [23]. They concluded that such fluidizing effect could favor the antioxidant capability and free radical scavenging characteristics of these compounds by making the interaction of antioxidant molecules with lipid radicals more efficient. Kaneko and co-workers have suggested that the protection of cells by phenolic antioxidants against cytotoxicity would be due to their incorporation rate into cell membranes due to their lipophilicity and to their orientation in biomembranes [24]. Furthermore, the antioxidant properties of silybin were suggested to be partially determined by its location at the lipid/water interface of cellular membranes [25]. In another work, quercetin and naringenin polyphenols, which are more effective against lipid autoperoxidation of rat cerebral membranes than they are against Fe^{2+}-induced oxidation, were found to be inserted deeper within phospholipid bilayers [26]. In comparison, another polyphenol called rutin elicits a stronger protective effect against the Fe^{2+}-induced oxidation of linoleate and it does not appear to interact with model membranes [26].

The interaction of cinnamic and *p*-coumaric acids with 1,2-dimyristoyl-*sn*-glycero-3-phosphocholine (DMPC) vesicles was investigated by using differential scanning calorimetry [27]. Interestingly, the *p*-coumaric acid was not able to modify significantly the thermotropic behavior of model membranes, and the cinnamic acid interacted with lipid vesicles at both neutral and acidic pHs. These differences were found to be essentially due to an additional hydroxyl group in the structure of the *p*-coumaric acid, as compared to the cinnamic acid, which resulted in less interaction with lipid membranes. The interaction with membranes was even reinforced for cinnamic acid at acidic pH, yielding a protonated form of the polyphenol that is then consequently more hydrophobic. Similarly, the penetration of quercetin in bilayers depends on the pH of the media. At acidic pH, quercetin is deeply embedded in planar lipid bilayers, while at physiological pH it interacts with the polar head groups at the water–lipid interface [28]. Ollila et al. showed an inverse correlation between the ability of polyphenols to induce membrane permeabilization (release of calcein entrapped in liposomes) and their retention on a chromatographic column coated with PC lipids [29]. Experiments with a series of flavonoids and different lipids, suggested that their interaction with membranes may rely on the establishment of hydrogen-bonds among the hydroxyl groups of the flavonoid and the polar headgroups of phospholipids [22,30].

In this study, we have chosen to investigate the antioxidant efficiency against lipid peroxidation of rosmarinic acid (RA, Fig. 1) and its interaction with lipid membranes. Among the molecules derived from phenolic acid, RA is a natural antioxidant found in many herbs of the Lamiaceae family such as rosemary, sage, lemon balm and thyme [31]. RA belongs to the family of hydroxycinnamic acids and it is an ester of 3,4-dihydroxyphenyllactic acid and caffeic acid [31]. The antioxidant activities of the yet-examined hydroxycinnamic acid derivatives can be ranked as follows: RA > chlorogenic acid > caffeic acid > ferulic acid > coumaric acid [32]. It is generally admitted that RA is an antioxidant as it may act as free radical scavenger [33–38] but RA also has a large number of other biological activities such as antiviral, antibacterial and anti-inflammatory properties and it could also prevent β-amyloid aggregation [31,39]. The interaction of RA with lipid membranes has been neither fully characterized [40,41] nor correlated to its antioxidant power. We have used liposomes composed of 1,2-dilinoleoyl-*sn*-glycero-3-phosphocholine (DLPC) to study the ability of RA to prevent lipid peroxidation and to quantify the amount of polyphenols that interacted with the lipid membrane. Moreover, the interaction of RA with different lipids was evidenced by using Langmuir monolayers. The organization of mixed DLPC/RA and 1,2-dipalmitoyl-*sn*-glycerol-3 phosphocholine (DPPC)/RA monolayers was investigated by atomic force microscopy (AFM) after transfer on mica substrate. The physico-chemical modifications of membrane properties induced by the interaction of RA were also studied by fluorescence with model liposomes. Finally, we have prepared DLPC/RA vesicles to evidence for the first time that the antioxidant protection of RA is directly due to its fraction spontaneously inserted within the membrane, with a percentage as low as ~1 mol%.

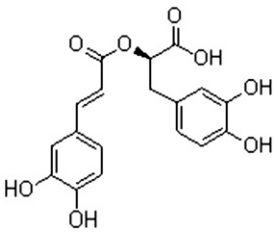

Fig. 1. Chemical structure of rosmarinic acid.

2. Material and methods

2.1. Chemicals

Rosmarinic acid (RA), 1,2-dipalmitoyl-*sn*-glycerol-3 phosphocholine (DPPC), 1,2-dilinoleoyl-*sn*-glycero-3-phosphocholine (DLPC), 1,2-dioleoyl-*sn*-glycero-3-phosphocholine (DOPC), 1-palmitoyl-2-oleoyl-*sn*-glycero-3-phosphocholine (POPC), 1-palmitoyl-2-oleoyl-*sn*-glycero-3-phosphoethanolamine (POPE), 1-palmitoyl-2-oleoyl-*sn*-glycero-3-phosphoserine (POPS), cholesterol (Chol), sphingomyelin from egg yolk (SM), 2,2′-azo-bis(2-amidinopropane) dihydrochloride (AAPH), 4-(2-Hydroxyethyl) piperazine-1-ethanesulfonic acid (Hepes) were purchased from Sigma (St. Louis, MO). Laurdan (6-dodecanoyl-2-dimethylaminonaphtalene) and Prodan (6-propionyl-2-dimethylaminonaphtalene) were from Molecular Probes (Eugene, Oregon). The water used in all assays was purified using a Millipore filtering system (Bedford, MA), yielding an ultrapure water (18.2 MΩ × cm). Stock solutions of pure phospholipids were prepared either with chloroform for the preparation of liposomes or with hexane/ethanol 9:1 (v/v) for the monolayer studies. RA was dissolved in ethanol and kept at −20 °C.

Log P values were calculated with the help of the software ChemDraw ultra v 7.0 (CambridgeSoft, 2003, Cambridge, UK).

2.2. Preparation of liposomes

Phospholipids alone or phospholipids/RA mixtures were dried under a stream of nitrogen and then kept under high vacuum for 2 h to obtain a solvent-free film. The dry film was then dispersed in Hepes buffer (10 mM Hepes, 150 mM NaCl pH 7.4) to produce multilamellar vesicles (MLVs). To prepare large unilamellar vesicles (LUVs), the MLVs were extruded 19 times through 200 nm nuclepore polycarbonate membrane filters (Avestin Inc. Ottawa, Canada) at 55 °C using a syringe-type extruder (Liposofast, Avestin Inc.). Small unilamellar vesicles (SUVs) were obtained by sonicating MLVs to clarity (3 cycles of 2 min 30 s) using a 500 W titanium probe sonicator (Fisher Bioblock Scientific, France; 33% of the maximal power; 13 mm probe diameter) while being kept in an ice bath. Then the liposome suspension was filtered on 0.2 μm Acrodisc® (Pall Life Sciences, USA) to remove titanium particles.

2.3. Antioxidant efficiency of RA

The antioxidant activity of RA was assessed by measuring the amount of conjugated dienes [42], which constitute the very first product of peroxidation for poly-unsaturated lipids [1,43]. These DLPC SUVs (0.5 mg/mL) prepared in Hepes buffer were mixed with different concentrations of RA prepared in Hepes (in the control assays, the liposomes were incubated with Hepes containing various

amounts of ethanol without RA). Then, the lipid peroxidation was initiated by adding 2 mM of AAPH, the peroxyl radical oxidizing agent to reach a final lipid concentration of 0.1 mg/mL. The samples were immediately incubated at 37 °C. Conjugated dienes were measured with a Specord S300 UV–VIS spectrophotometer (Jena, Germany) at 234 nm. Results were expressed as percentages of peroxidation after 60 min of peroxidation [38,41], calculated as follows [44]:

$$\%\ peroxidation = \left(Abs_{sample} / Abs_{control}\right) \times 100.$$

A control experiment was also performed by recording the absorbance at 234 nm of a solution of RA at 60 μM oxidized by 2 mM of AAPH in Hepes buffer. No significant modification of the absorbance was measured.

2.4. Membrane partitioning of RA

To quantify the insertion of RA in lipid membranes, we have followed the protocol described by Nakayama et al. [45]. Briefly, different concentrations of RA were added to a solution of DLPC SUVs at a final concentration of 1 mg/mL. After incubation for 20 min at 20 °C, the mixture was centrifuged at 200,000 *g* for 20 min with a Beckman Air-Driven Ultracentrifuge (Beckman, Fullerton, CA, U.S.A.). The pellets were resuspended with 1 mL of ethanol. The amount of RA in the ethanolic solution was measured by injecting 20 μL of the sample solution on an HPLC LC 1200 equipped with a UV detector (Agilent Technologies, Massy, France). We have used a C18 reverse-phase column (Uptisphere WOD C18 column, 5 μm, 250 mm × 4.6 mm, Interchim, Montluçon, France). The elution was performed by injecting a mobile phase containing acetonitrile:water 30:70 (v/v) at a flow rate of 0.5 mL/min and the wavelength for detection was 280 nm. The concentration of RA was calculated from a calibration curve prepared with standard solutions. Lipids in the pellet were quantified by the method developed by Stewart [46]. The RA/lipid mol ratio was calculated for each concentration of RA tested.

2.5. Monolayer studies

All the experiments were performed at constant temperature (21 ± 0.1 °C). The film balance was built by KSV (Minitrough 2, KSV Instruments Ltd, Helsinki, Finland) for pressure area isotherms and by NIMA (NIMA Technology, England) for adsorption experiments on a small Teflon dish. Both the minitrough and the dish were equipped with a Wilhelmy-type pressure measuring system. In these experiments, the subphase was Hepes buffer and it was continuously stirred with a magnetic stirrer spinning at 100 rpm.

2.5.1. Adsorption of RA at constant surface area

Adsorption experiments were performed on a Teflon dish (surface = 19.6 cm²) with a subphase volume of 62 mL. Phospholipids were spread at the air–water interface in hexane/ethanol 9:1 (v/v) to reach the desired surface pressure. As soon as the initial surface pressure was stabilized (~15 min), RA solubilized in ethanol was injected into the subphase to a final concentration of 15 μM using a Hamilton syringe. RA adsorption at the air–water interface was then followed by measuring the variations in surface pressure. A control experiment was also performed by injecting ethanol alone in the subphase, which produced no significant perturbation of the surface pressure.

2.5.2. Pressure/area (π–A) isotherms and Langmuir–Blodgett transfer of monolayers

The Langmuir trough from KSV was equipped with two moveable Teflon barriers permitting to compress lipid monolayers at the air–water interface. At their most opened position, the surface available to spread lipids between the two barriers was 75 × 252 mm², and the subphase volume was 200 mL. Lipids alone or mixed with RA were spread in hexane/ethanol 9:1 (v/v) at the air–water interface. The solvent was allowed to evaporate for 15 min before compression. The monolayer was then compressed at 10 mm²/min up to 30 mN/m. After stabilization, the monolayers were transferred onto freshly cleaved mica supports by vertically raising the supports through the air–water interface at a rate of 5 mm/min.

2.6. AFM imaging

Supported monolayers were investigated using a commercial AFM (NanoScope III MultiMode AFM, Veeco Metrology LLC, Santa Barbara, CA) equipped with a 125 μm × 125 μm × 5 μm scanner (J-scanner). Topographic images were recorded in contact mode at room temperature (~21 °C) and in air using oxide-sharpened microfabricated Si_3N_4 cantilevers (Microlevers, Veeco Metrology LLC, Santa Barbara, CA) with spring constants ranging from 0.01 to 0.1 N/m (manufacturer specified), with a minimal applied force (<200 pN) and at a scan rate of 5 Hz. The curvature radius of silicon nitride tips was ~20 nm. All images (256 × 256 pixels) shown in this paper are flattened raw data.

2.7. Laurdan and Prodan fluorescence

Laurdan and Prodan generalized polarization (GP) was determined in SUVs of DPPC alone or with 1 mol% of RA. Stock solutions of Laurdan (1 mmol/L) and Prodan (1 mmol/L) were prepared in ethanol. The final concentrations of the probes in the samples were: 1 μmol/L Laurdan and 3 μmol/L Prodan. Laurdan and Prodan were excited at 360 nm. GP was calculated according to the following equation given by Parasassi et al. [47]:

$$GP = (I_B - I_R) / (I_B + I_R).$$

Fluorescence emission intensity of a blue edge of the spectrum (I_B) was measured at 435 nm for Laurdan and 440 nm for Prodan; fluorescence intensity of a red spectrum edge (I_R) was recorded at 490 nm for Laurdan and 480 nm for Prodan; using a Varian Cary Eclipse fluorescence spectrophotometer (Victoria, Australia), equipped with a thermoregulated cell holder. The intrinsic fluorescence of RA was verified at the emission wavelengths of the two probes and the values we found were not significant.

The Laurdan probe is a lipophilic dye able to insert within membranes with its naphthalene moiety located just below the headgroups of lipids, among their glycerol backbone, while the linear hydrophobic dodecanoyl tail of Laurdan is embedded within the acyl chains of the lipids. Light excitation of Laurdan molecules modifies their dipole moment, which leads to a reorientation of water molecules that are surrounding the dye's naphthalene moiety embedded at the headgroups/hydrophobic core interface of lipid membranes. On the emission spectrum, such orientation of water molecules with the Laurdan's dipole leads to a red shift of the probe's emission. This phenomenon is even more important with increasing amounts of water molecules around the dye. So, in lipid membranes, the Laurdan probe is sensitive to the amount of water molecules present within the bilayer. Finally, variations in membrane water content provoke red shifts in the Laurdan emission spectrum, which can be quantified by calculating the GP value. If the lipids are well-ordered, water molecules will have less access to the Laurdan probes embedded in the membrane, thus resulting in a high value of GP. In membranes with lower order, the GP will decrease as result of a greater access of water to the Laurdan probe inside the lipid bilayer [48].

In contrast to Laurdan, Prodan preferentially partitions in the fluid phase and is sensitive to the pretransition of polar heads. These two probes are sensitive to polarity variations occurring in the bilayer, but because of their different hydrophobicities, Prodan detects variations close to the bilayer surface, and Laurdan measures variations more deeply in the membrane [49,50].

2.8. Calcein release

The ability of RA to permeabilize liposomes was measured with the calcein release assay. LUVs encapsulating the fluorescent probe were prepared as described above except for the hydration of the lipid film that was done in Hepes buffer containing 35 mM calcein. Then, free calcein was separated from encapsulated calcein by gel filtration on a sepharose 4B column equilibrated with Hepes buffer. Lipids were quantified with the method developed by Stewart [46]. The calcein-loaded liposomes were diluted to a final concentration of 10 μM lipids in Hepes buffer. Fluorescence measurements were performed at room temperature immediately after the RA addition with Varian Cary Eclipse fluorescence spectrophotometer (Victoria, Australia) using excitation and emission wavelengths of 490 and 520 nm respectively. The intrinsic fluorescence of RA at 520 nm was verified and the value we found was not significant.

3. Results and discussion

3.1. Antioxidant efficiency of RA against lipid peroxidation

To investigate the antioxidant ability of RA against the AAPH-mediated peroxidation of lipids, we have prepared SUVs containing phospholipids with poly-unsaturated chains, DPLC. These preformed vesicles were then mixed with different amounts of exogenously added RA and they were finally incubated at 37 °C with the hydrophilic radical generator: AAPH. After different times of incubation with AAPH, the absorbance of conjugated dienes formed in lipid molecules was measured at 234 nm to assess lipid peroxidation [42] (Fig. 2A). In the control experiment, the absorbance at 234 nm was measured for AAPH-treated liposomes, but this time without RA (Fig. 2A). Fig. 2A revealed that the absorbance at 234 nm increased with time except for the control experiment that reached a plateau after 30 min. This plateau may be explained by compensation between the decomposition and formation rates of hydroperoxides [42]. The percentage of peroxidation for each concentration of RA was deduced from the control experiment and was plotted versus time (Fig. 2B). As one can see for all the RA concentrations tested, the percentage of peroxidation increased with time. After 60 min, the DLPC was fully peroxidized for RA at 0.25 μM whereas the peroxidation level was lower than 20% for concentrations of RA higher than 2 μM. The percentage of peroxidation calculated at 60 min was plotted against the RA concentration (Fig. 2C). This curve confirms that the percentage of peroxidation decreased with increasing amounts of RA exogenously added to preformed vesicles. With this curve, we have determined the concentration of RA that inhibited the peroxidation in DLPC liposomes by 50% (IC_{50}): 1.51 ± 0.05 μM.

Altogether, these results showed the high efficiency of RA to prevent the lipid peroxidation induced by the hydrophilic radical generator AAPH. However, two hypotheses could explain this antioxidant effect: (i) RA molecules in the bulk phase could have stopped the propagation of the free radical before they have reached the lipids, and/or (ii) RA molecules associated with the lipid membrane could have blocked the propagation of free radicals within the bilayer (either by modifying the membrane fluidity or by scavenging the free radicals). Such mechanisms were previously proposed for other polyphenols able to interact with lipid membranes [22].

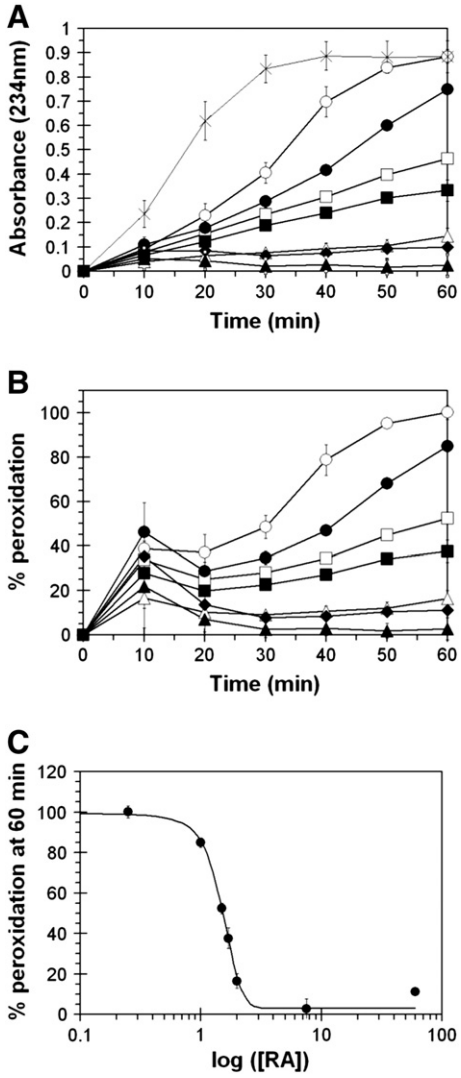

Fig. 2. Antioxidant activity of RA against AAPH-induced oxidation of DLPC liposomes. DLPC liposomes preformed in Hepes buffer at 0.1 mg/mL were mixed with different concentrations of RA: 0.25 μM (open circles); 1 μM (closed circles); 1.5 μM (open squares); 1.7 μM (closed squares); 2 μM (open triangles); 7.5 μM (closed triangles) and 60 μM (closed diamonds). A control experiment was realized by mixing DLPC SUVs in Hepes buffer at 0.1 mg/mL with 2 mM of AAPH (cross). AAPH was then added at 2 mM to generate hydrosoluble radicals. After different times of incubation at 37 °C, conjugated dienes were measured at 234 nm (A). Results (from three independent experiments) were expressed as percentages of peroxidation and plotted versus time (B). The percentage of peroxidation obtained at 60 min was plotted versus the concentration of RA (C). These data points were fitted with a dose–response curve with variable Hill slope using the OriginPro 8.5 software.

3.2. Quantification of the RA amount associated with the membrane of DLPC liposomes

The ability of RA to associate with lipid vesicles was also determined. SUVs incubated with different amounts of RA were subjected to centrifugation and the pellets were analyzed by HPLC (Fig. 3). Fig. 3 shows that the RA/lipid molar ratio increased with the amount of RA initially added to the liposomes. These experimental points were fitted with a Langmuir equation to determine the theoretical saturation of the lipid membrane with RA molecules. The Langmuir equation used was as follows:

$$A = A_{max} \times K \times [RA] / (1 + K \times [RA])$$

where A is the RA/lipid molar ratio. This fit of the data points permitted to determine the maximum RA/lipid molar ratio Amax equal to 1.033% and K which is the Langmuir equilibrium constant equal to 18.57 μM. In a recent paper, Londono-Londono and coworkers studied the incorporation of two flavonoids in DMPC membranes: hesperidin (HD) and hesperetin (HT) [51]. They observed that the liposomes were close to saturation with these flavonoids at molar ratios of 0.38% and 2.08% for HD and HT, respectively. According to the log P of each compound (−0.48 and 2.44 for HD and HT, respectively), the difference in the

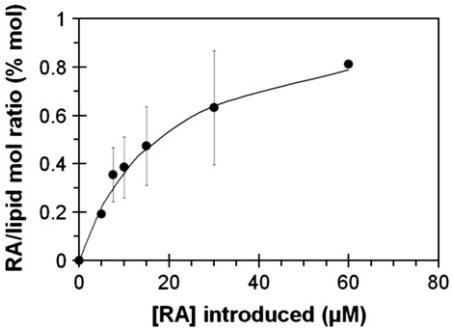

Fig. 3. Quantification of RA inserted into DLPC liposomes. DLPC liposomes prepared in Hepes buffer at 1 mg/mL were incubated with different concentrations of RA. After centrifugation, the pellets were resuspended in ethanol and the lipids were quantified by the Stewart method [46]. Finally, the RA associated with liposomes was quantified by HPLC. The RA/lipid molar ratio was calculated for each concentration of RA tested. All the results are expressed as mean ± standard deviation (n = 3). Experimental data points were fitted to a Langmuir equation by using the OriginPro 8.5 software (see Results and discussion).

incorporation was related to the higher lipophilicity of HT compared to HD. The log P of RA was found to be 2.07, which means that RA has a lipophilicity higher than HD but lower than HT. Thus, it is not surprising to obtain a molar ratio of incorporation for RA at 1.033%, which is below the HT/lipid mol ratio but above the HD/lipid one.

3.3. Interaction of RA with lipid monolayers at different surface pressures

We have shown that RA is able to interact with PC in vesicles. To gain a view on the lipid selectivity of RA insertion into membranes, we have used the Langmuir technique. Indeed, with this technique, we can form monolayers of lipids that are not able to organize alone into vesicles (i.e. without a lipid such as PC forming lamellar phases) due to their molecular shape [52]. Monolayers of the different lipids were spread at the air–water interface of a small Teflon dish with constant surface area. After stabilization at the desired initial surface pressure (π_0), the RA was injected into the subphase at 15 μM final concentration, and the variation of pressure was recorded along with time (inset in Fig. 4). For all the lipids, the injection of RA into the subphase provoked an immediate increase of the surface pressure. After saturation of the pressure versus time curve, the $\Delta\pi$ (difference between the initial and the final pressures) was plotted as a function of π_0 (Fig. 4). By extrapolating the regression lines to a $\Delta\pi$ equal to zero, we have determined the maximum insertion pressure (MIP) for each lipid or lipid mixtures (Table 1). Considering the three lipids DPPC, DOPC and POPC, the MIP value followed the rank order DOPC > POPC > DPPC. According to this result, RA insertion seems to be dependent on the amount of unsaturations in lipid chains. The level of unsaturation is directly correlated to the order of acyl chains: more unsaturations increase lipid disorder [53]. This means that the insertion of RA within lipid monolayers is dependent on the molecular packing. It is worth noting that for DLPC the MIP was lower (58.5 mN/m) than the one obtained for DOPC.

If we compare the influence of the polar headgroup of lipids on the penetration capacity of RA, it seems that RA is less able to penetrate the negatively charged headgroup of PS lipids (MIP = 48.5 mN/m) as compared with PC (58.0 mN/m). This result is not surprising because at pH 7.4 RA bears a negative charge (carboxylate group) that may cause charge repulsion between the two carboxylate functions of the serine in PS. The MIP of POPE is also considerably lower than that of POPC, which can be attributed to higher molecular hindrance of PE headgroups that are more hydrated than the PC ones [54].

The MIP value for SM monolayers was high: 60.0 mN/m whereas it was only 33.0 mN/m for Chol. The MIP value of POPC and SM monolayers was strongly decreased by adding 30% of Chol to these phospholipids. These results clearly show that the penetration of RA is more difficult in the monolayers that are rigidified by Chol molecules.

Most importantly, it is noteworthy that the MIP was always higher than 30 mN/m regardless of lipid composition except for Chol. If we consider that 30 mN/m corresponds to the internal pressure of biological membranes [55], it means that exogenously added RA is spontaneously able to insert into natural lipid membranes, except for domains enriched in Chol.

As suggested in the review by Calvez et al. [56], the MIP values are sometimes not sufficient to interpret the data, $\Delta\pi$ values can provide additional information. Thus, from each regression curve obtained by plotting $\Delta\pi$ versus π_0, we have checked the values of $\Delta\pi$ obtained at the π_0 corresponding to the internal pressure of natural membranes (π_0 = 30 mN/m; see Table 1). As one can see for the pure lipids, the $\Delta\pi_{30mN/m}$ values followed the rank order: DOPC = SM > DLPC > POPC > DPPC > POPE > POPS > Chol. The MIP value permits to predict if a molecule will be able to penetrate a natural lipid bilayer and the $\Delta\pi_{30mN/m}$ is more informative of the amount of RA inserted in the membrane. Indeed, high $\Delta\pi_{30mN/m}$ values may correspond to high amounts of RA inserted in the membrane. These results evidence the high affinity of RA for zwitterionic lipid bearing several unsaturations (DOPC and DLPC) and for SM. It is again worth noting that according to the low $\Delta\pi_{30mN/m}$ value obtained with the Chol monolayer (0.5 mN/m), Chol enriched membranes may resist to RA penetration. According to Oteiza et al. [22], the interaction of the hydrophilic

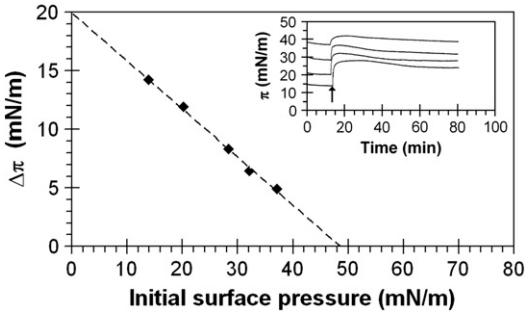

Fig. 4. Penetration of RA into DPPC monolayers. DPPC was spread at the air–Hepes interface to reach different initial surface pressures. After stabilization (~15 min), the RA (15 μM, see arrow in the inset) was injected in the subphase. As a result, the surface pressure increased (inset) due to insertion of RA in the monolayer. The variation of surface pressure was then plotted as a function of the initial pressure. The subphase was Hepes buffer at 21 °C.

Table 1
Maximum insertion pressures of RA injected at a final concentration of 15 μM under different lipid monolayers. The MIP value was obtained by extrapolating the regression lines to the x-axis (see Fig. 3). The $\Delta\pi_{30mN/m}$ represents the $\Delta\pi$ at 30 mN/m initial surface pressure and it was calculated from the equation of the regression lines obtained in the $\Delta\pi = f(\pi_0)$ plots. The subphase was always Hepes buffer at 21 °C.

	MIP (mN/m)	$\Delta\pi_{30mN/m}$ (mN/m)
DPPC	48.6	7.6
DOPC	65.9	8.3
POPC	58.0	7.8
POPE	50.7	6.1
POPS	48.5	5.0
SM	60.0	8.3
Chol	33.0	0.5
POPC/Chol 7:3 (mol/mol)	54.0	9.5
SM/Chol 7:3 (mol/mol)	55.0	5.9
DLPC	58.5	8.1

flavonoids with the polar headgroups of lipids is mainly associated with the formation of hydrogen bonds. It is well known that SM molecules can form abundant hydrogen bonds between their polar heads [57,58], then the formation of hydrogen bonds between SM and RA might explain the high values of $\Delta\pi_{30mN/m}$ and MIP obtained.

3.4. Surface morphology of mixed RA/lipid monolayers

To visualize the modifications of the DLPC and DPPC membranes due to the insertion of 1% RA, mixtures of DLPC/RA and DPPC/RA (99:1 molar ratios) were spread at the air/water interface and compressed up to 30 mN/m, which correspond to the internal pressure of natural lipid membranes [55]. Then, the monolayers were transferred onto mica and imaged in air by AFM. Representative images of DPPC monolayers transferred at 30 mN/m are shown in Fig. 5A and B. At this surface pressure, DPPC monolayers are in the liquid condensed (LC) phase, as a result they present only one gray level on AFM images. Concerning the DPPC/RA monolayers, the images reveal two distinct levels (Fig. 5C and D). The height difference between these two levels is 1.0 ± 0.1 nm, which is consistent with the coexistence of liquid expanded (LE) and LC phases [59,60]. At 30 mN/m, DLPC monolayers are in the LE phase and no LC domains are visible (data not shown). After the addition of RA into the DLPC monolayer, no modification of the surface morphology was observed (data not shown). These results clearly evidence the ability of RA to reside preferentially in the LE phase in the DPPC monolayers at 30 mN/m. However, it should be noticed that apparently the presence of 1% RA, the amount of polyphenol able to insert spontaneously in the lipid bilayers, did not modify significantly membrane structure and integrity.

3.5. Influence of RA on the fluidity of DPPC liposomes

The fluorescent probes Laurdan and Prodan were employed to study not only the influence of RA on the order of DPPC molecules in bilayers but also to assess the depth at which RA molecules reside in the membrane. It is worth noting that Laurdan mainly probes modifications of lipid order in the hydrophobic part of the membrane, in contrast with Prodan that measures lipid order at the interface between the acyl chains and the polar heads in the membrane [49,50,61,62]. DPPC was chosen because this lipid exhibits a phase transition from gel to fluid state at 41 °C [63] allowing then to study the influence of RA on both the gel and the fluid phases of the lipid. By fitting these points, one can determine the inflection point which indicates the lipid main phase transition (Tm). The GP profiles for DPPC SUVs alone are very similar to previously published results obtained under similar conditions [61,62].

As shown in Fig. 6A, 1 mol% of RA did not influence the Laurdan fluorescence significantly in the temperature range studied. The Tm of DPPC remained unchanged in the presence of the polyphenol. So, it seems that RA does not affect the order of lipids in DPPC membranes. This result is consistent with the findings of Perez-Fons et al. [40]. Indeed, they observed by differential scanning calorimetry that adding 15 mol% of RA to DMPC liposomes has no effect on the transition from gel to fluid phase. With the Prodan probe (Fig. 6B), one can observe that adding 1 mol% of RA to DPPC liposomes led to significant changes of the lipid order among the headgroups. Indeed, below the Tm, the GP of DPPC liposomes was slightly decreased by the presence of the polyphenol in the membrane, and above the Tm the GP was strongly increased. These results are consistent with an association of RA molecules near the polar headgroups of the lipids. Furthermore, the slight decrease of the GP value below the Tm of DPPC traduces a decrease in the lipid order which is consistent with the higher amount of LE phase observed in the AFM images with 1 mol% RA in DPPC. For temperatures above the Tm of DPPC, the GP increase can be attributed to an increase of the membrane order due to the insertion of RA molecules among the polar headgroups of lipids. Silybin was shown to interact with the DPPC polar headgroups and to strongly influence the DPPC pre-transition by decreasing the GP values below the Tm [62].

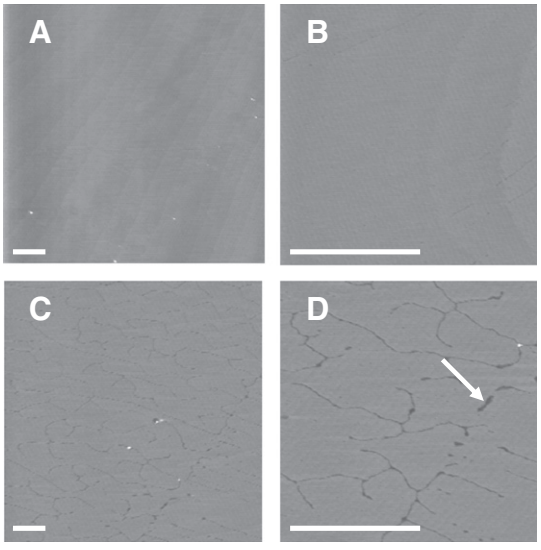

Fig. 5. AFM height images of DPPC and DPPC/RA monolayers transferred at 30 mN/m. Pure monolayers of DPPC (A and B), and DPPC/RA 99:1 mol/mol (C and D) were transferred on mica at 30 mN/m to be imaged in air by AFM. The subphase was Hepes buffer at a constant temperature of 21 °C. The z-scale is 5 nm for all images and the scale bars are 2.5 μm. The white arrow in panel D points at a domain of the monolayer in the LE phase.

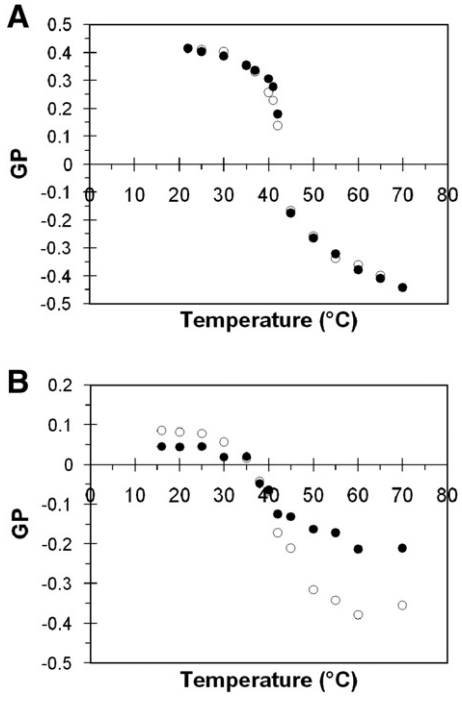

Fig. 6. Influence of RA on membrane fluidity. Generalized polarization (GP) of the Laurdan (A) and Prodan (B) fluorescent probes were plotted as a function of temperature for SUVs of DPPC without (open symbols) or with 1 mol% RA (closed symbols). The final concentrations of lipids, Laurdan and Prodan probes were 110, 1 and 3 μM, respectively. These data points were fitted with a dose/response curve with variable Hill slope using the OriginPro 8.5 software.

3.6. Calcein leakage studies

The influence of RA on the integrity of lipid membrane was investigated using the calcein leakage assay. To this end, calcein was encapsulated into LUVs at a concentration that was high enough (35 mM) to provoke the self-quenching of the fluorescent probe. Under these conditions, the permeabilization of LUVs' membrane would lead to a release of the calcein, which will result in the dilution of the probe and a dequenching responsible for an increase of fluorescence intensity. Whatever the initial RA concentration added (up to 1 mM) to LUVs, no fluorescence increase was obtained indicating that no modification of the membrane permeability occurred with this polyphenol. This result indicates that exogenously added RA is not able to destabilize lipid membranes even at high concentrations.

3.7. Influence of RA penetration in membranes for the prevention of lipid peroxidation

It is clear that the maximal amount of RA that can spontaneously enter DLPC membranes is only 1 mol%. This raises the questions of (i) the minimal amount of inserted RA that is necessary to inhibit efficiently lipid peroxidation and (ii) of the influence of RA in the bulk medium on lipid peroxidation. These important points were examined by introducing different amounts of RA in the organic solution of lipids before the drying step yielding solvent-free lipid films. As a result, the DLPC vesicles were loaded with controlled amounts of RA. The molar percentages of RA chosen were ranging between 0.2 and 1 mol% because 1.033 mol% was determined to be the maximum percentage of RA associated with the vesicles (Fig. 3). The percentages of peroxidation measured for SUVs of DLPC containing RA in their membrane were plotted versus the DLPC/RA molar ratio introduced in the membrane (Fig. 7). This curve exhibits a sigmoidal shape showing that at contents of membrane-inserted RA higher than 0.4 mol%, the percentage of peroxidation decreased importantly. By fitting these points, we have determined the $IC_{50} = 0.52 \pm 0.04$ mol%. With the data from Fig. 3, we can calculate the theoretical percentage of RA that may penetrate the membrane for every concentration of exogenous RA added to vesicles. The curve with the closed symbols in Fig. 7 represents the percentage of peroxidation plotted as a function the calculated RA/lipid molar ratio associated with the lipid membrane.

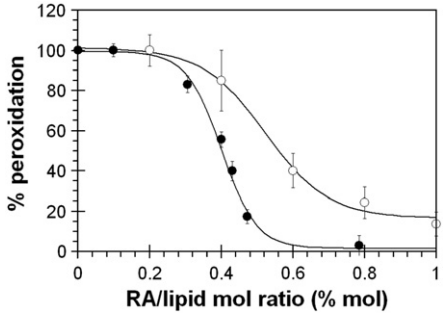

Fig. 7. Antioxidant activity of membrane inserted RA against AAPH-induced oxidation of DLPC liposomes. Liposomes composed of different molar ratios of DLPC/RA were prepared in Hepes buffer at 0.1 mg/mL. AAPH was then added at 2 mM to initiate the generation of hydrosoluble radicals. After different incubation times at 37 °C, conjugated dienes were measured at 234 nm. Results were expressed as percentages of peroxidation after 60 min and plotted versus the lipid/RA molar ratios (open circles). The theoretical lipid/RA molar ratios were calculated from the data shown in Figs. 2 and 3 for all the concentrations of RA added to preformed liposomes. The percentage of peroxidation obtained at 60 min was plotted versus the theoretical lipid/RA molar ratios (closed circles). All the results are expressed as mean ± standard deviation (n = 3). Experimental data points were fitted to a sigmoidal dose/response curve with variable Hill slope using the OriginPro 8.5 software.

As one can see, the experimental curve and the theoretical one are very similar ($IC_{50} = 0.40 \pm 0.01$ mol%). This result suggests that RA is able to prevent lipid peroxidation mainly when it is inserted in the membrane. The difference in the IC_{50} determined experimentally and by extrapolation might be due to a very small fraction of RA in the bulk phase that could help in preventing lipid peroxidation. In a recent paper [41], the IC_{50} of RA was determined with the Thiobarbituric Acid-Reactive Substances (TBARS) assay by using eggPC SUVs and AAPH as a free radical generator. They obtained a value of IC_{50} at ~3 μM which is in the same range as the value of 1.51 μM obtained when RA was exogenously added to preformed liposomes. However, this IC_{50} is overestimated because RA is partitioned between the membrane and the bulk phase. In fact, the RA fraction that is effective in preventing lipid peroxidation seems to be exclusively the one incorporated inside the membrane.

4. Conclusions

In this work, we have shown that RA is an efficient antagonist of lipid peroxidation. We have also evidenced that this polyphenol is able to insert spontaneously in lipid membranes, with a higher affinity for unsaturated than for saturated lipids. We have determined a maximum RA/lipid molar ratio of insertion of ~1%. A more detailed analysis permitted to show that RA is able to reside in the membrane, most likely in the portion that is close to the headgroups of lipids, a region that is accessible to polar molecules such as hydrosoluble radicals from the bulk phase. The insertion of 1 mol% of RA was not sufficient to promote significant alterations of the membrane structure and fluidity. Most importantly, for the first time, we demonstrate that a small amount of RA is able to insert spontaneously inside membranes, and this fraction of RA is efficiently able to prevent lipid peroxidation.

Moreover, Chol-rich membranes were found to be resistant to the insertion of RA. In fact, RA molecules could protect plasma membranes of mammal cells efficiently against lipid oxidation, but they will be excluded from the regions enriched in Chol such as lipid rafts.

Acknowledgements

The financial support of the Centre National de la Recherche Scientifique (CNRS), of the French Ministry of Research, of the Université de Technologie de Compiègne (UTC, Plan de Pluriformation «Assemblages Biomimétiques — PPF BIOMIM»), and of the Région Picardie is gratefully acknowledged. The authors thank the Service d'Analyse Physico-Chimique (SAPC) of the UTC for providing AFM facilities. Special thanks to Dr Slim Azouzi for fitting experimental data.

References

[1] B. Halliwell, J.M. Gutteridge, Role of free radicals and catalytic metal ions in human disease: an overview, Methods Enzymol. 186 (1990) 1–85.
[2] L. Gate, J. Paul, G.N. Ba, K.D. Tew, H. Tapiero, Oxidative stress induced in pathologies: the role of antioxidants, Biomed. Pharmacother. 53 (1999) 169–180.
[3] A. Tonks, R.H. Morris, A.J. Price, A.W. Thomas, K.P. Jones, S.K. Jackson, Dipalmitoylphosphatidylcholine modulates inflammatory functions of monocytic cells independently of mitogen activated protein kinases, Clin. Exp. Immunol. 124 (2001) 86–94.
[4] J.H. Exon, E.H. South, Effects of sphingomyelin on aberrant colonic crypt foci development, colon crypt cell proliferation and immune function in an aging rat tumor model, Food Chem. Toxicol. 41 (2003) 471–476.
[5] P. Kuo, M. Weinfeld, J. Loscalzo, Effect of membrane fatty acyl composition on LDL metabolism in Hep G2 hepatocytes, Biochemistry 29 (1990) 6626–6632.
[6] M.L. Tomassoni, D. Amori, M.V. Magni, Changes of nuclear membrane lipid composition affect RNA nucleocytoplasmic transport, Biochem. Biophys. Res. Commun. 258 (1999) 476–481.
[7] T.G. Niranjan, T.P. Krishnakantha, Membrane changes in rat erythrocyte ghosts on ghee feeding, Mol. Cell. Biochem. 204 (2000) 57–63.
[8] M. Hashimoto, M.S. Hossain, T. Shimada, H. Yamasaki, Y. Fujii, O. Shido, Effects of docosahexaenoic acid on annular lipid fluidity of the rat bile canalicular plasma membrane, J. Lipid Res. 42 (2001) 1160–1168.

[9] H. Kuhn, A. Borchert, Regulation of enzymatic lipid peroxidation: the interplay of peroxidizing and peroxide reducing enzymes, Free Radic. Biol. Med. 33 (2002) 154–172.
[10] X. Wang, P.J. Quinn, Vitamin E and its function in membranes, Prog. Lipid Res. 38 (1999) 309–336.
[11] H. Girao, C. Mota, P. Pereira, Cholesterol may act as an antioxidant in lens membranes, Curr. Eye Res. 18 (1999) 448–454.
[12] S. Morandat, M. Bortolato, G. Anker, A. Doutheau, M. Lagarde, J.P. Chauvet, B. Roux, Plasmalogens protect unsaturated lipids against UV-induced oxidation in monolayer, Biochim. Biophys. Acta 1616 (2003) 137–146.
[13] J. Zhang, R.A. Stanley, L.D. Melton, Lipid peroxidation inhibition capacity assay for antioxidants based on liposomal membranes, Mol. Nutr. Food Res. 50 (2006) 714–724.
[14] L.O. Dragsted, Antioxidant actions of polyphenols in humans, Int. J. Vitam. Nutr. Res. 73 (2003) 112–119.
[15] R. Beliveau, D. Gingras, Role of nutrition in preventing cancer, Can. Fam. Physician 53 (2007) 1905–1911.
[16] W. Guo, E. Kong, M. Meydani, Dietary polyphenols, inflammation, and cancer, Nutr. Cancer 61 (2009) 807–810.
[17] C.G. Fraga, M. Galleano, S.V. Verstraeten, P.I. Oteiza, Basic biochemical mechanisms behind the health benefits of polyphenols, Mol. Aspects Med. 31 (2010) 435–445.
[18] A.B. Hendrich, Flavonoid–membrane interactions: possible consequences for biological effects of some polyphenolic compounds, Acta Pharmacol. Sin. 27 (2006) 27–40.
[19] V.R. de Lima, M.P. Morfim, A. Teixeira, T.B. Creczynski-Pasa, Relationship between the action of reactive oxygen and nitrogen species on bilayer membranes and antioxidants, Chem. Phys. Lipids 132 (2004) 197–208.
[20] B.M. Fahlman, E.S. Krol, Inhibition of UVA and UVB radiation-induced lipid oxidation by quercetin, J. Agric. Food Chem. 57 (2009) 5301–5305.
[21] S. Gal, D. Lichtenberg, A. Bor, I. Pinchuk, Copper-induced peroxidation of phosphatidylserine-containing liposomes is inhibited by nanomolar concentrations of specific antioxidants, Chem. Phys. Lipids 150 (2007) 186–203.
[22] P.I. Oteiza, A.G. Erlejman, S.V. Verstraeten, C.L. Keen, C.G. Fraga, Flavonoid–membrane interactions: a protective role of flavonoids at the membrane surface? Clin. Dev. Immunol. 12 (2005) 19–25.
[23] M.E. Gutierrez, A.F. Garcia, M. Africa de Madariaga, M.L. Sagrista, F.J. Casado, M. Mora, Interaction of tocopherols and phenolic compounds with membrane lipid components: evaluation of their antioxidant activity in a liposomal model system, Life Sci. 72 (2003) 2337–2360.
[24] T. Kaneko, K. Kaji, M. Matsuo, Protection of linoleic acid hydroperoxide-induced cytotoxicity by phenolic antioxidants, Free Radic. Biol. Med. 16 (1994) 405–409.
[25] T. Parasassi, A. Martellucci, F. Conti, B. Messina, Drug–membrane interactions: silymarin, silibyn and microsomal membranes, Cell Biochem. Funct. 2 (1984) 85–88.
[26] A. Saija, M. Scalese, M. Lanza, D. Marzullo, F. Bonina, F. Castelli, Flavonoids as antioxidant agents: importance of their interaction with biomembranes, Free Radic. Biol. Med. 19 (1995) 481–486.
[27] F. Castelli, N. Uccella, D. Trombetta, A. Saija, Differences between coumaric and cinnamic acids in membrane permeation as evidenced by time-dependent calorimetry, J. Agric. Food Chem. 47 (1999) 991–995.
[28] L. Movileanu, I. Neagoe, M.L. Flonta, Interaction of the antioxidant flavonoid quercetin with planar lipid bilayers, Int. J. Pharm. 205 (2000) 135–146.
[29] F. Ollila, K. Halling, P. Vuorela, H. Vuorela, J.P. Slotte, Characterization of flavonoid–biomembrane interactions, Arch. Biochem. Biophys. 399 (2002) 103–108.
[30] S.V. Verstraeten, C.L. Keen, H.H. Schmitz, C.G. Fraga, P.I. Oteiza, Flavan-3-ols and procyanidins protect liposomes against lipid oxidation and disruption of the bilayer structure, Free Radic. Biol. Med. 34 (2003) 84–92.
[31] M. Petersen, M.S. Simmonds, Rosmarinic acid, Phytochemistry 62 (2003) 121–125.
[32] M.A. Soobrattee, V.S. Neergheen, A. Luximon-Ramma, O.I. Aruoma, T. Bahorun, Phenolics as potential antioxidant therapeutic agents: mechanism and actions, Mutat. Res. 579 (2005) 200–213.
[33] J.H. Chen, C.-T. Ho, Antioxidant activities of caffeic acid and its related hydroxycinnamic acid compounds, J. Agric. Food Chem. 45 (1997) 2374–2378.
[34] Y. Nakamura, Y. Ohto, A. Murakami, H. Ohigashi, Superoxide scavenging activity of rosmarinic acid from *Perilla frutescens* Britton Var. *acuta* f. *viridis*, J. Agric. Food Chem. 46 (1998) 4545–4550.
[35] C. Jayasinghe, N. Gotoh, T. Aoki, S. Wada, Phenolics composition and antioxidant activity of sweet basil (*Ocimum basilicum* L.), J. Agric. Food Chem. 51 (2003) 4442–4449.
[36] B. Tepe, O. Eminagaoglu, H.A. Akpulat, E. Aydin, Antioxidant potentials and rosmarinic acid levels of the methanolic extracts of *Salvia verticillata* (L.) subsp. *verticillata* and *S. verticillata* (L.) subsp. *amasiaca* (Freyn & Bornm.) Bornm, Food Chem. 100 (2007) 985–989.
[37] B. Tepe, Antioxidant potentials and rosmarinic acid levels of the methanolic extracts of *Salvia virgata* (Jacq), *Salvia staminea* (Montbret & Aucher ex Bentham) and *Salvia verbenaca* (L.) from Turkey, Bioresour, Technology 99 (2008) 1584–1588.
[38] J. Alamed, W. Chaiyasit, D.J. McClements, E.A. Decker, Relationships between free radical scavenging and antioxidant activity in foods, J. Agric. Food Chem. 57 (2009) 2969–2976.
[39] T. Hamaguchi, K. Ono, A. Murase, M. Yamada, Phenolic compounds prevent Alzheimer's pathology through different effects on the amyloid-beta aggregation pathway, Am. J. Pathol. 175 (2009) 2557–2565.
[40] L. Perez-Fons, F.J. Aranda, J. Guillen, J. Villalain, V. Micol, Rosemary (*Rosmarinus officinalis*) diterpenes affect lipid polymorphism and fluidity in phospholipid membranes, Arch. Biochem. Biophys. 453 (2006) 224–236.
[41] L. Perez-Fons, M.T. Garzon, V. Micol, Relationship between the antioxidant capacity and effect of rosemary (*Rosmarinus officinalis* L.) polyphenols on membrane phospholipid order, J. Agric. Food Chem. 58 (2010) 161–171.
[42] R.A. Wheatley, Some recent trends in the analytical chemistry of lipid peroxidation, Trends Anal. Chem. 19 (2000) 617–628.
[43] E. Schnitzer, I. Pinchuk, D. Lichtenberg, Peroxidation of liposomal lipids, Eur. Biophys. J. 36 (2007) 499–515.
[44] C. Hu, Y.V. Yuan, D.D. Kitts, Antioxidant activities of the flaxseed lignan secoisolariciresinol diglucoside, its aglycone secoisolariciresinol and the mammalian lignans enterodiol and enterolactone in vitro, Food Chem. Toxicol. 45 (2007) 2219–2227.
[45] T. Nakayama, K. Ono, K. Hashimoto, Affinity of antioxidative polyphenols for lipid bilayers evaluated with a liposome system, Biosci. Biotechnol. Biochem. 62 (1998) 1005–1007.
[46] J.C. Stewart, Colorimetric determination of phospholipids with ammonium ferrothiocyanate, Anal. Biochem. 104 (1980) 10–14.
[47] T. Parasassi, G. De Stasio, A. d'Ubaldo, E. Gratton, Phase fluctuation in phospholipid membranes revealed by Laurdan fluorescence, Biophys. J. 57 (1990) 1179–1186.
[48] S.A.T.M.A. Sanchez, G. Gunther, E. Gratton, Laurdan generalized polarization: from cuvette to microscope. Modern research and educational topics in microscopy, in: A. Méndez-Vilas, J. Díaz (Eds.), , 2007, pp. 1007–1014.
[49] E.K. Krasnowska, E. Gratton, T. Parasassi, Prodan as a membrane surface fluorescence probe: partitioning between water and phospholipid phases, Biophys. J. 74 (1998) 1984–1993.
[50] T. Parasassi, E.K. Krasnowska, L. Bagatolli, E. Gratton, Laurdan and Prodan as polarity-sensitive fluorescent membrane probes, J. Fluoresc. 8 (1998) 365–373.
[51] J. Londono-Londono, V.R. Lima, C. Jaramillo, T. Creczynski-Pasa, Hesperidin and hesperetin membrane interaction: understanding the role of 7-O-glycoside moiety in flavonoids, Arch. Biochem. Biophys. 499 (2010) 6–16.
[52] J.N. Israelachvili, Intermolecular and Surface Forces, Academic Press, London, 1991.
[53] N. Anton, P. Saulnier, F. Boury, F. Foussard, J.P. Benoit, J.E. Proust, The influence of headgroup structure and fatty acyl chain saturation of phospholipids on monolayer behavior: a comparative rheological study, Chem. Phys. Lipids 150 (2007) 167–175.
[54] M. Dyck, P. Kruger, M. Losche, Headgroup organization and hydration of methylated phosphatidylethanolamines in Langmuir monolayers, Phys. Chem. Chem. Phys. 7 (2005) 150–156.
[55] D. Marsh, Lateral pressure in membranes, Biochim. Biophys. Acta 1286 (1996) 183–223.
[56] P. Calvez, S. Bussieres, E. Demers, C. Salesse, Parameters modulating the maximum insertion pressure of proteins and peptides in lipid monolayers, Biochimie 91 (2009) 718–733.
[57] B. Ramstedt, J.P. Slotte, Membrane properties of sphingomyelins, FEBS Lett. 531 (2002) 33–37.
[58] E. Mombelli, R. Morris, W. Taylor, F. Fraternali, Hydrogen-bonding propensities of sphingomyelin in solution and in a bilayer assembly: a molecular dynamics study, Biophys. J. 84 (2003) 1507–1517.
[59] S. Azouzi, K. El Kirat, S. Morandat, The potent antimalarial drug cyclosporin A preferentially destabilizes sphingomyelin-rich membranes, Langmuir 26 (2010) 1960–1965.
[60] P.E. Milhiet, C. Domec, M.C. Giocondi, N. Van Mau, F. Heitz, C. Le Grimellec, Domain formation in models of the renal brush border membrane outer leaflet, Biophys. J. 81 (2001) 547–555.
[61] T. Parasassi, G. De Stasio, G. Ravagnan, R.M. Rusch, E. Gratton, Quantitation of lipid phases in phospholipid vesicles by the generalized polarization of Laurdan fluorescence, Biophys. J. 60 (1991) 179–189.
[62] O. Wesolowska, B. Lania-Pietrzak, M. Kuzdzal, K. Stanczak, D. Mosiadz, P. Dobryszycki, A. Ozyhar, M. Komorowska, A.B. Hendrich, K. Michalak, Influence of silybin on biophysical properties of phospholipid bilayers, Acta Pharmacol. Sin. 28 (2007) 296–306.
[63] R.L. Biltonen, D. Lichtenberg, The use of differential scanning calorimetry as a tool to characterize liposome preparation, Chem. Phys. Lipids 64 (1993) 129–142.